SUPPLEMENTAL FIGURES

Figure S1. Genotype analysis of Pum-myc *Drosophila* DL1 cells.
(A) PCR-based genotyping of the DL1 Pum-myc cells confirmed homozygous insertion of the myc epitope tag. Pum exon 13 was PCR amplified from genomic DNA isolated from wild type DL1 cells in comparison to the Pum-myc clonal isolate. The gel image was cropped to show the relevant lanes, as indicated by the dashed vertical line.
(B) Sequence chromatogram of exon 13 of the Pum gene from the Pum-myc DL1 clonal line. The sequencing confirms insertion of a human rhinovirus (HRV) 3C protease site and myc epitope tag onto the C-terminus of the Pum coding sequence (CDS).

Figure S1
Haugen et al.

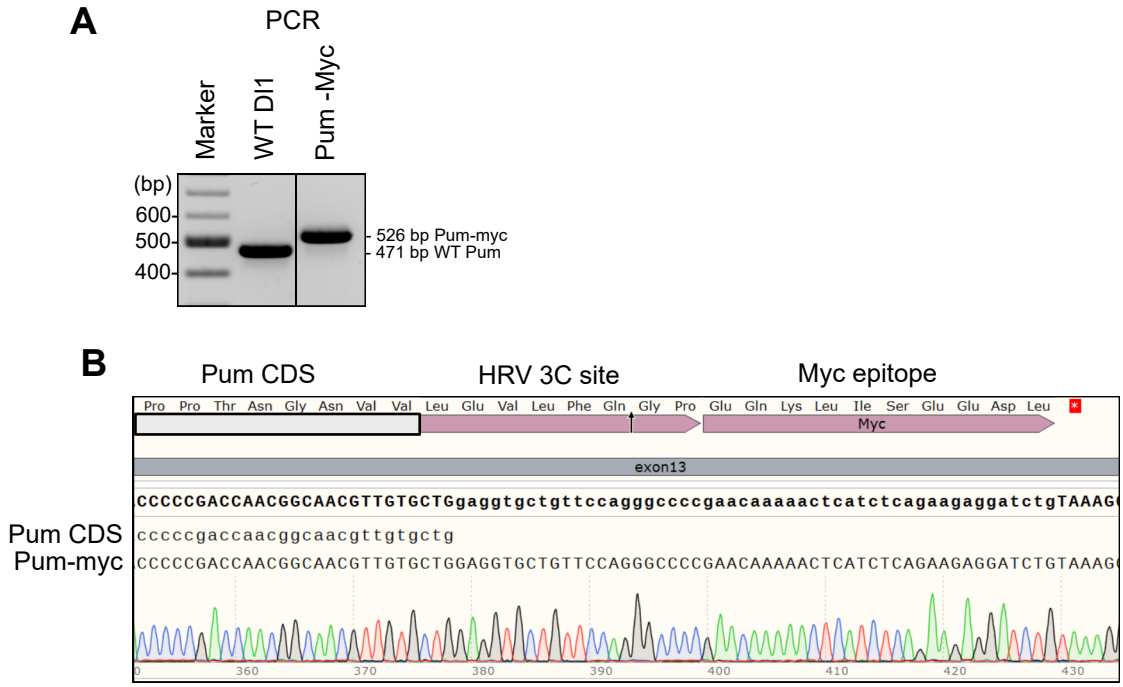

Figure S2. Enrichment sequence motifs in Pum KO + Pum, Pop2, and Not1 RNAi RNA-Seq datasets. RNA-sequence motifs significantly correlated with changes in transcript abundance, as measured in the Click-Seq datasets, were identified using FIRE. The distribution of transcript Wald statistic values was set in 9 discretized bins, and the over- or under-representation of the identified motif in each bin is indicated by the blue-yellow color scale at the top. Significantly over-represented motifs in the corresponding datasets are shown on the right. Z-scores, output by FIRE, indicate the information content of the optimized motif. The E-value output by TOMTOM indicates how confidently the motif matched with a known RNA-binding protein.

Figure S2
Haugen et al.

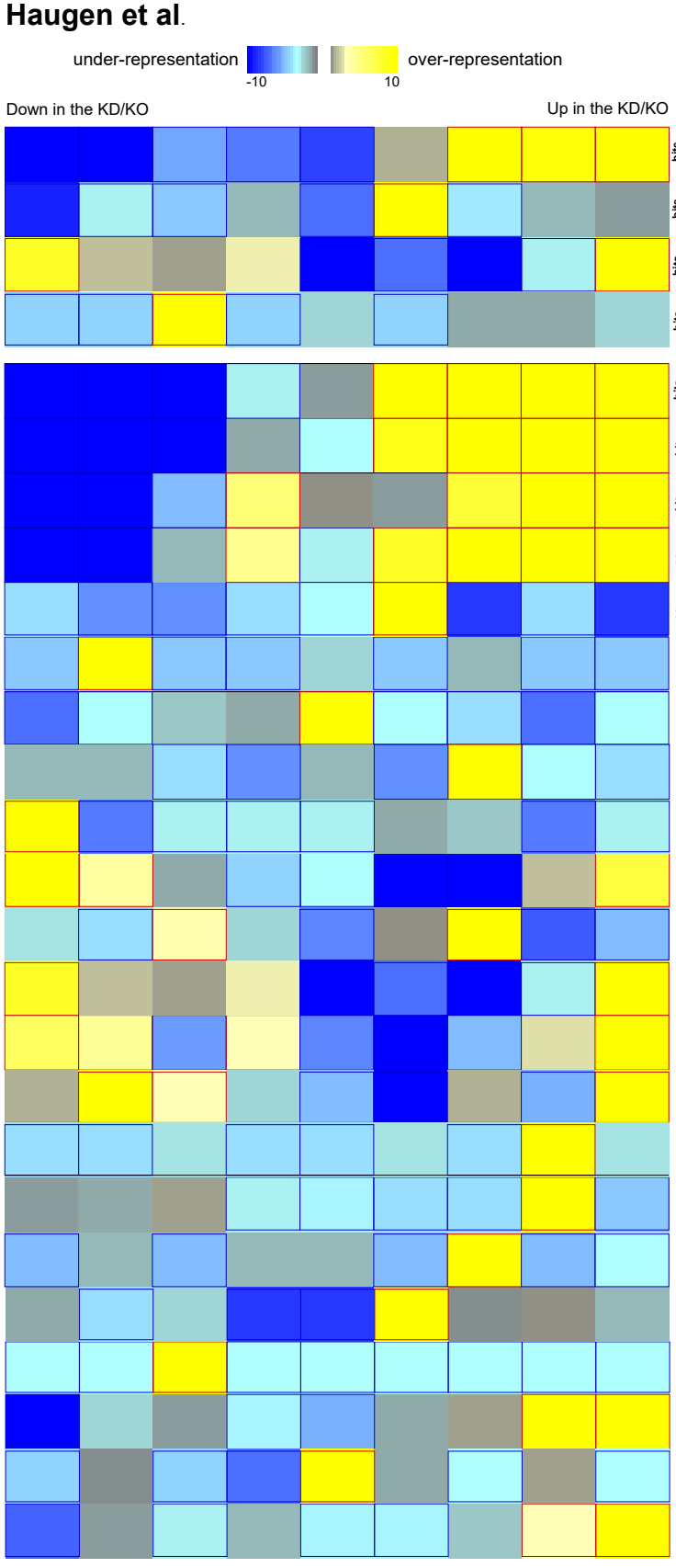

Optimized Motif	Z-score	E-value	RBP name	Dataset
	166.2	1.41E-05	Pum	RNAi Pum 3'
	82.3	0.0334057 / 0.0361353	Hrb98DE / Hrb87F	RNAi Pop2 5'
	67.7	0.0368714	Pabp2	KO1 Pum 5'
	55.3	0.0153394	B52	KO1 Pum 3'
	274.4			RNAi Not1 5'
	259.4			RNAi Not1 3'
	157.1			RNAi Pop2 5'
	145.3			RNAi Pop2 3'
	128.8			RNAi Not1 5'
	77.8			KO1 Pum 5'
	77.3			KO2 Pum 5'
	74.9			RNAi Pum 5'
	72.8			KO2 Pum 5'
	72.5			KO2 Pum 3'
	69.0			RNAi Pum 3'
	67.7			KO1 Pum 5'
	67.5			KO1 Pum 3'
	63.2			KO2 Pum 5'
	63.0			RNAi Pum 5'
	61.4			RNAi Pum 3'
	60.8			RNAi Pop2 3'
	60.3			RNAi Not1 3'
	59.1			KO1 Pum 5'
	58.2			KO1 Pum 5'
	53.6			KO2 Pum 3'
	50.8			KO1 Pum 5'

Figure S3. Genotype analysis of Pum knockout *Drosophila* DL1 cells, Pum KO1.
(A) Diagram of the Pumilio coding region depicting the location of the CRISPR-Cas9 targeted region and primer sets used for PCR, sequencing, and RT-qPCR detection. Pumilo repression domains (RD1-3), conserved motifs A and B, and RNA binding domain (RBD) are labeled.
(B) Exon 9 of the Pumilio (Pum) gene was PCR amplified in wild type DL1 and Pumilio KO1 clonal DL1 cell lines. The gel image was cropped to show the relevant lanes, as indicated by the dashed vertical line.
(C) The products in B were sequenced to confirm the wild type and Pumilio KO1 genotype, as shown by the aligned chromatograms. The position of the single guide RNA used for CRISPR-Cas9 genome engineering is shown at the top, along with the protospacer adjacent motif (PAM). The 81 base pair insertion and 20 base pair deletion in the Pumilio KO1 is highlighted.
(D) Diagram of the Pumilio protein produced Pumilio KO1 cell line. The combined insertion and deletion results in a net gain of 61 base pairs. The resulting frameshift after glutamine 725 in this mutant pumilio protein adds 8 amino acids (shown in red) followed by a stop codon, resulting in a 733 amino acid non-functional protein product that lacks domains PCMb, RD3, and RBD.
(E) RT-qPCR analysis, using primer sets in exon 9 and exon 11 as shown in panel A, measured the reduction of Pum mRNA in the Pumilio KO1 relative to the wild type DL1 cells. Mean $\log_2$ fold change values are reported. N=3

Figure S3
Haugen et al.

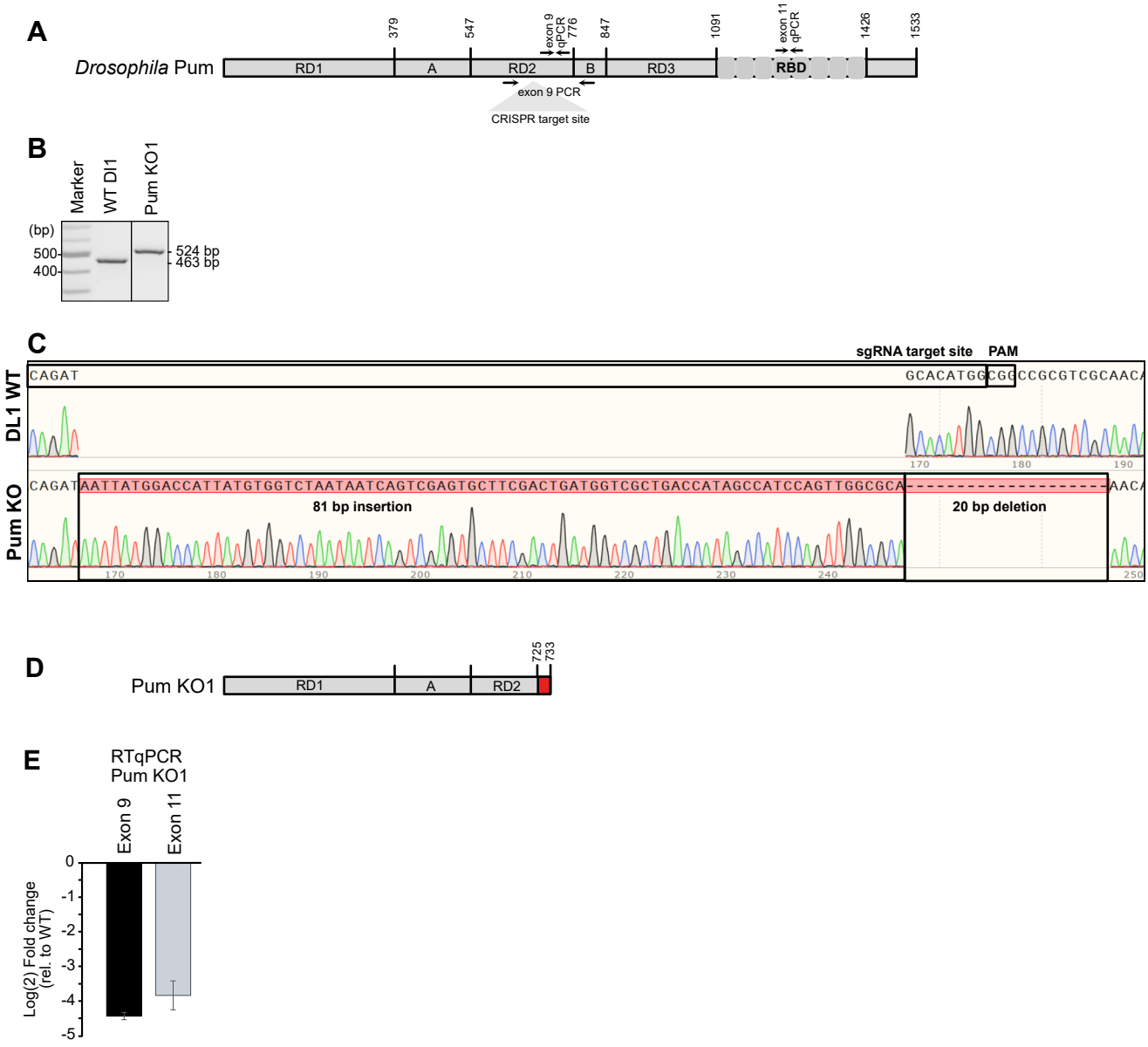

Figure S4. Identification of differentially expressed genes in response to knockout of Pum in two clonal lines of *Drosophila* DL1 cells. Volcano plots of statistical significance (q-value) versus mean $\log_2$ fold change of RNA levels in Pum KO1 **(A)** and KO2 **(B)** clonal lines relative to wild type DL1 cells, measured by RNA-seq. Vertical dashed lines indicate a $\log_2$ fold change value of +/- $\log_2(1.3)$. A statistical significance threshold (q-value ≤ 0.05) is shown with a horizontal dashed line. Red or blue markers ("x") indicate genes passing both statistical significance and fold change thresholds in positive (Up) or negative (Down) directions, respectively. Plot of mean normalized RNA-Seq read counts per kilobase of Pum KO1 **(A)** and Pum KO2 **(B)** clonal lines versus wild type DL1 cells. Significantly upregulated and downregulated genes are highlighted as red and blue points, respectively.

Figure S4
Haugen et al.

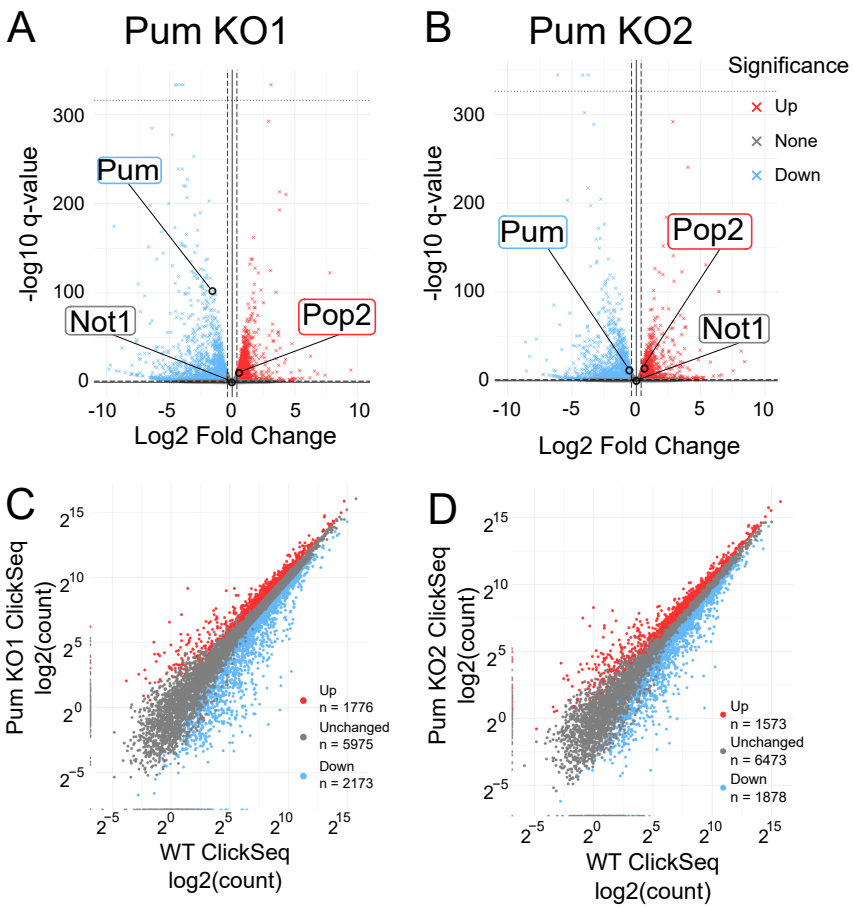

Figure S5. Genotype analysis of V5-Raf in DL1 Pum-myc cells.
(A) PCR-based genotyping of the V5-tagged Raf gene in DL1 Pum-myc cells confirmed homozygous insertion of the V5 tag. Raf exon 3 was PCR amplified from genomic DNA isolated from parental Pum-myc DL1 cells in comparison to the V5-Raf clonal isolate.
(B) Sequence chromatogram of exon 3 of the Raf gene from the V5-Raf DL1 Pum-myc clonal line. The sequencing confirms insertion of the V5 tag onto the N-terminus of the Raf coding sequence (CDS), maintaining the natural 5′UTR and translation initiation codon.

Figure S5
Haugen et al.

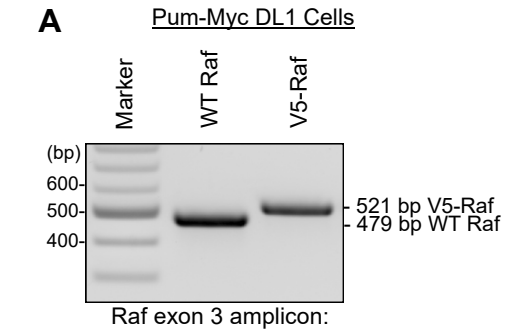

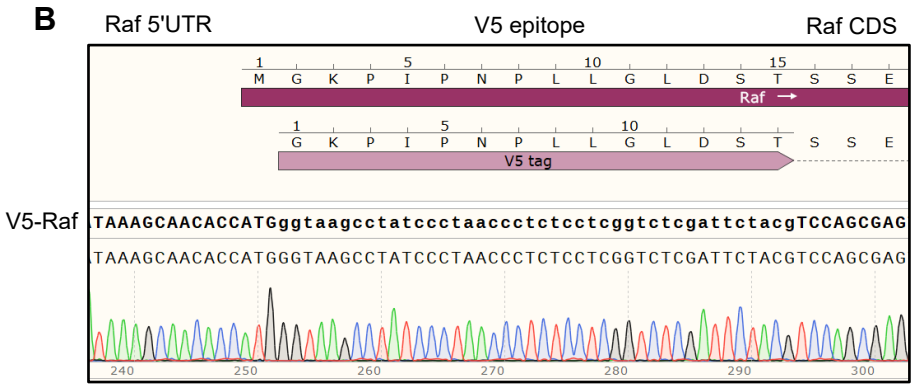

Figure S6. Gene ontology analysis of differentially expressed transcripts in response to Not1 knockdown relative to negative control RNAi (NTC). This chart is an expanded version of Figure 5B. GO terms showing significant mutual information with the observed $\log_2$ fold changes upon Not1 knockdown, measured in our RNA-seq dataset. The $\log_2$ fold changes were discretized into 5 equally populated bins, ranging from downregulated on the left (Down in KD) to upregulated on the right (Up in KD). GO terms showing significant mutual information, calculated using iPAGE, are listed on the right. The color of each cell shows the magnitude of the P-value for significance of the enrichment (red) or depletion (blue) at that cell, scale is shown on the left side of the figure; black bordered cells individually show P-values ≤ 0.05 after Bonferroni correction across their row.

Figure S6
Haugen et al.

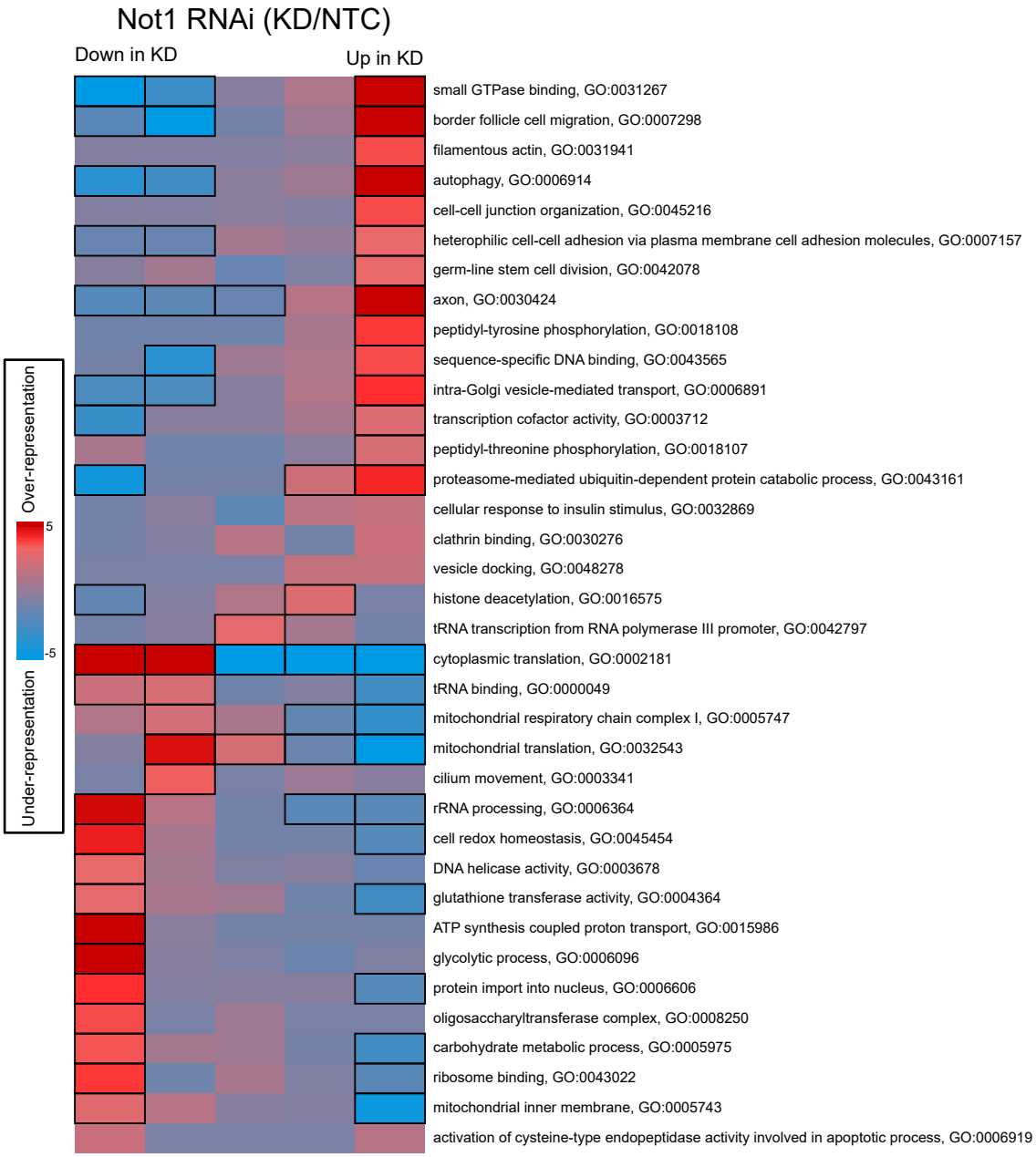

Figure S7. Gene ontology analysis of differentially expressed transcripts in response to Pop2 knockdown relative to negative control RNAi (NTC). This chart is an expanded version of Figure 5B. GO terms showing significant mutual information with the observed $\log_2$ fold changes upon Pop2 knockdown, measured in our RNA-seq dataset. The $\log_2$ fold changes were discretized into 5 equally populated bins, ranging from downregulated on the left (Down in KD) to upregulated on the right (Up in KD). GO terms showing significant mutual information, calculated using iPAGE, are listed on the right. The color of each cell shows the magnitude of the P-value for significance of the enrichment (red) or depletion (blue) at that cell, scale is shown on the left side of the figure; black bordered cells individually show P-values ≤ 0.05 after Bonferroni correction across their row.

Figure S7
Haugen et al.

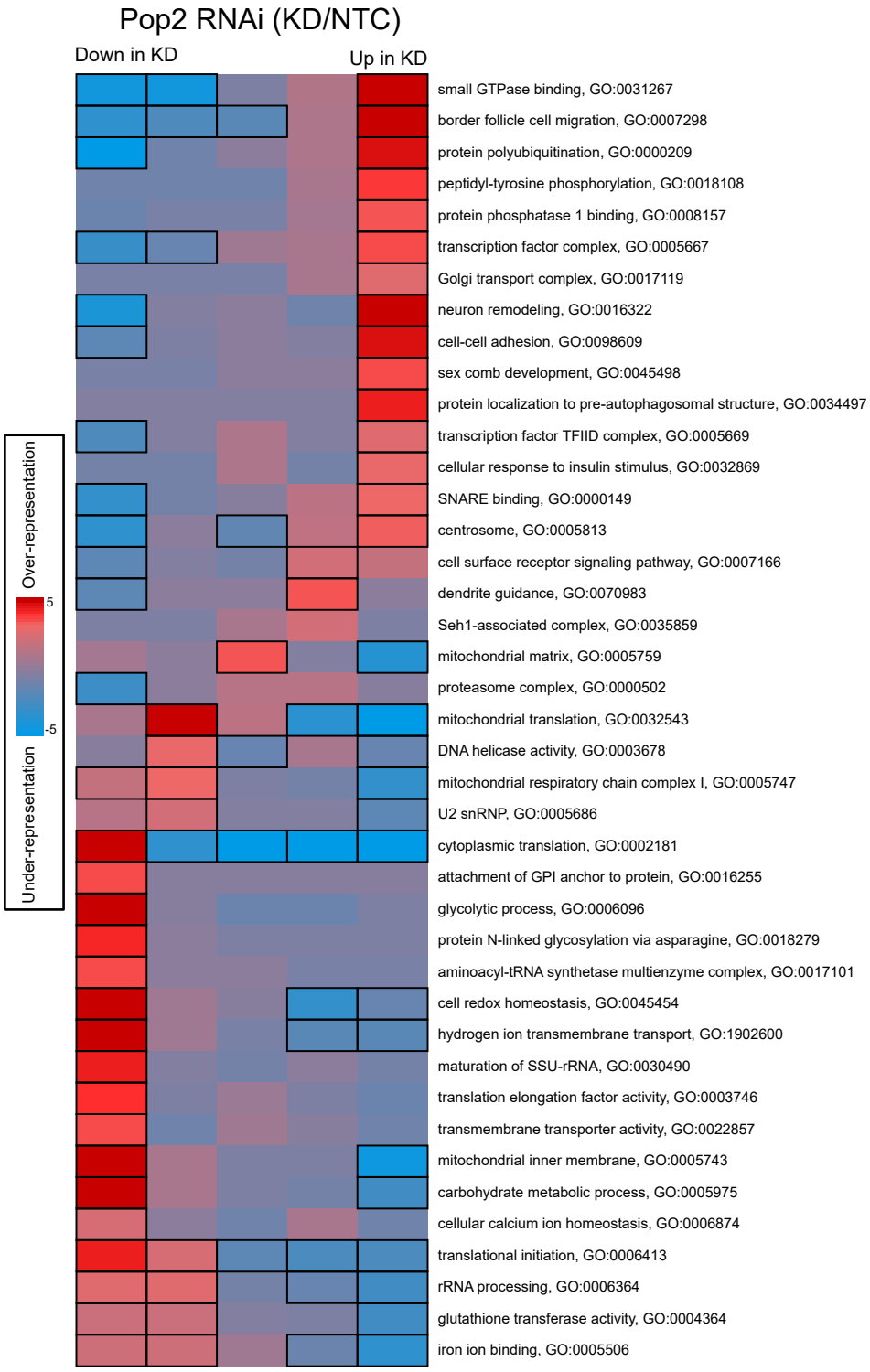

Figure S8. Relationship of transcript abundance and codon optimality.
Density distributions as violin plots of $\log_{10}$ mean normalized count per Kb for transcripts binned by codon optimality. Transcript abundances were measured by RNA-Seq in the negative control NTC treated DL1 cells. Density medians are indicated with black lines within each violin.

Figure S8
Haugen et al.